Long-Range Inhomogeneities in Sulfonated Polystyrene Ionomers

Yingjie Li,† Dennis G. Peiffer,‡ and Benjamin Chu*,†

Department of Chemistry, State University of New York at Stony Brook, Long Island, New York 11794-3400, and Corporate Research Science Laboratory, Exxon Research and Engineering Company, Clinton Township, Route 22 East, Annandale, New Jersey 08801

Received March 1, 1993; Revised Manuscript Received May 4, 1993

ABSTRACT: Two Bonse–Hart ultra-small-angle X-ray scattering (USAXS) cameras were constructed and calibrated by using a polystyrene latex suspension and laser light scattering. The instruments were used to investigate the long-range inhomogeneities in a series of sulfonated polystyrene ionomers. The USAXS measurements were mainly centered in the region of $q<0.1$ nm^{-1} (where q is the magnitude of the scattering vector), which is beyond the reach of most conventional small-angle X-ray scattering (SAXS) instruments. All the scattering profiles of ionomers showed a small-angle upturn which was much higher than their parent pure polystyrene. The scattering behavior in this q region was not strongly dependent upon the counterions (except for the intensity change in amplitude), the compression-molding condition, temperature, and annealing. The small-angle upturn decreased with increasing ionic content for zinc sulfonated polystyrene ionomers, and increased with increasing ionic content for rubidium sulfonated polystyrene ionomers. By means of the Debye–Bueche model, an inhomogeneity length of around tens of nanometers was detected in the usual q range accessible by conventional SAXS (0.045–0.12 nm^{-1}). However, the USAXS curves based on the Debye–Bueche model showed a consistent downward curvature in the light-scattering q range. A Guinier plot also failed to show a simple characteristic length. Surprisingly, the upturn could better be described by a power law $I\sim q^{-\alpha}$, with α ranging from 2.4 to 3.6 for the ionomers in this study, suggesting that, in the absence of long-range order, the structure could be very polydisperse and irregular. On the basis of USAXS results, the origin of the upturn is discussed. The majority of the upturn could result from chemical compositional inhomogeneities of the ionomers and the processing procedures used in forming the ionomer films for various physical measurements such as SAXS.

Introduction

Many physical properties of organic polymers can be improved by introducing a small amount of ionic groups to the polymers. This class of materials, known as ionomers, has been a topic of intense research efforts.[1-6] It is important to study the structural changes and to understand the structure–property relationship for this class of polymers. Although a variety of techniques, particularly small-angle X-ray scattering (SAXS), has provided experimental evidence that the ionic groups form aggregates, the exact shape, size, and spatial arrangement of the ionic groups are still uncertain. Generally, SAXS of ionomers shows an ionic peak located in the region of q = 1–3 nm^{-1} where q is the magnitude of the scattering vector and $q = (4\pi/\lambda)\sin(\theta/2)$, with λ and θ being the X-ray wavelength and the scattering angle, respectively. The lack of structure in the limited q range means that such scattering profiles can be represented by many models. For example, the core–shell model by MacKnight et al.[7] suggested that the peak was due to intraparticle interference. The liquidlike model by Yarusso and Cooper[8] suggested that it was due to interparticle interference. Although the liquidlike model was more successful in representing the ionic peak, it could not explain the upturn at very small q values. Recently, there have been some attempts to fit both the peak and the upturn by using a single model.[9,10] These models have been reviewed by Register[11] and by Visser and Cooper.[9] In practice, it is difficult to prove the uniqueness of a model and the difficulty increases with the number of parameters in the model.

Although the small-angle upturn could be related directly to the ionic peak,[12-18] its profile in the very small q range ($q<0.05$ nm^{-1}) could not be ascertained because of the low q limit in conventional SAXS instruments. Yarusso and Cooper[8] first attributed the small-angle upturn (or upturn) to artifacts, such as parasitic scattering, void, neutralizing agent, or other impurities. However, from anomalous SAXS experiments, Ding et al.[14] and Chu et al.[15,18] found that the upturn was due to the metal cations and considered a likely origin to be the inhomogeneous distribution of these cations without specifying their states, e.g., ion pairs, multiplets, clusters, or a combination of them. Earlier, Williams et al.[12] assumed the upturn to be due to an inhomogeneous distribution of multiplets. Galambos et al.[13] attributed the upturn to a spatial arrangement of the ionic groups by showing that annealing of the solution-cast sulfonated polystyrene ionomer decreased the intensity of the upturn, while it increased the intensity of the ionic peak. Moore et al.[17] showed that the intensity of the upturn relative to the intensity of the ionic peak decreased as the degree of alkylation was increased.

Williams et al.,[12] Ding et al.,[14] Chu et al.,[15,18] and Register and Cooper[16] all tried to use the Debye–Bueche model to analyze their upturn data. The fitting by Chu et al.[15] showed a consistent curvature from $q\sim0.03$ nm^{-1}, which was by far the lowest accessible q value reported for ionomers by using a conventional SAXS instrument. Kumar and Pineri[19] showed that scattering from a sample with uniform electron density but finite volume could also yield an upturn. However, the calculated intensity from this source was considerably smaller than the experimentally observed values.[14]

Recently, Eisenberg et al.[20] proposed a new model to explain the mechanical properties of ionomers. The ionic peak was attributed to the prevalent intermultiplet distance within the clusters, which were assumed to be highly irregular. On the basis of this model, the upturn could be attributed, at least in part, to the spatial distribution of the clusters. As the clusters could be related directly to the mechanical properties of the ionomers,[20] it should be highly desirable to learn more about the origin

* To whom correspondence should be addressed.
† State University of New York at Stony Brook.
‡ Exxon Research and Engineering Co.

0024-9297/93/2226-4006$04.00/0

of the upturn by covering a smaller q range not accessible by conventional SAXS instruments.

We have developed a room-temperature Bonse–Hart ultra-small-angle X-ray scattering (USAXS) camera[21] and a high-temperature USAXS camera,[22] employing both synchrotron and conventional X-ray sources. The instruments could reach a very small q value of ≤ 0.004 nm^{-1}, which is more than 1 order of magnitude smaller than that of most conventional SAXS instruments. In a previous Communication,[23] we reported the feasibility of using our room-temperature Bonse–Hart USAXS camera to study the upturn of ionomers.

It should be noted that the Bonse–Hart camera employing synchrotron radiation does not exactly follow the infinite-slit-length geometry, while the Bonse–Hart camera employing a conventional X-ray source is close to an infinite-slit-length geometry. Thus, the results employing a synchrotron source contain higher uncertainties at high q values. In this study, we used our Bonse–Hart USAXS instruments to determine the upturn and its dependence upon metal cations, ionic content, sample preparation method, temperature, and annealing in order to seek a deeper understanding of the origin of the upturn. Both synchrotron and conventional X-ray sources were used.

Experimental Section

Materials. Monodisperse polystyrene standards were purchased from Polysciences. The sulfonation of polystyrenes and the neutralization (100%) by metal salts were carried out following the procedures described in ref 24. The samples are denoted by M-SPS-xx where M, SPS, and xx represent cation, sulfonated polystyrene, and sulfonation level (mol %), respectively. Unless specified, the samples were compression-molded at 200 °C and then cooled to room temperature in ~3 min. The parent polystyrene in Na-SPS-10.9 has a M_n of $\sim 6.0 \times 10^5$ and a molecular weight distribution index M_w/M_n of 1.06. The parent polystyrene in Rb-SPS-11.4 has a M_n of $\sim 9.0 \times 10^5$ and a M_w/M_n of 1.10. The parent polystyrene in Rb-SPS-13.0 has a M_n of $\sim 6.0 \times 10^5$ and a M_w/M_n of 1.06. The parent polystyrene in Zn-SPS samples has a M_n of $\sim 1.05 \times 10^5$ and a M_w/M_n of 1.02.

Room-Temperature Bonse–Hart USAXS Camera. The details of the room-temperature Bonse–Hart camera have been described in ref 21. We used two channel-cut germanium crystals with 6 reflections each. It took about 30 min to get one typical USAXS curve with a synchrotron source and about 10 h with a rotating-anode X-ray generator source. We found no essential difference between th two setups. However, the setup using the focused synchrotron X-ray beam did not seem to obey the infinite-slit-length geometry at high q values. Figure 1a shows the test results by using a Dow Chemical "monodisperse" polystyrene latex suspension with a volume fraction of 3.2% in a 1:2 (v/v) water/ethanol mixed solvent. The synchrotron USAXS experiment was performed at the SUNY X3A2 beamline, National Synchrotron Light Source (NSLS), Brookhaven National Laboratory (BNL).

Most literature reported the calibration of Bonse–Hart cameras by using dried latex spheres. However, quantitative calibration cannot be made because of the particle–particle interference effect. In Figure 1a, we used a dilute suspension of latex spheres. Then the structure factor could be corrected according to Vrij et al.[25] A comparison between the model curve and the USAXS curve clearly shows the high resolution of our instrument.

We paid more attention to the performance of the camera in the small q region by comparing the USAXS result with the laser light scattering (LLS) result. Figure 1b shows that our Bonse–Hart camera can reach a low q range which is comparable to that from LLS, while, at the same time, the camera can reach much higher q values than those accessible by LLS. Parts a and b of Figure 1 represent, to our knowledge, the first quantitative calibration of a Bonse–Hart camera, since data treatment for USAXS and LLS is quite different.

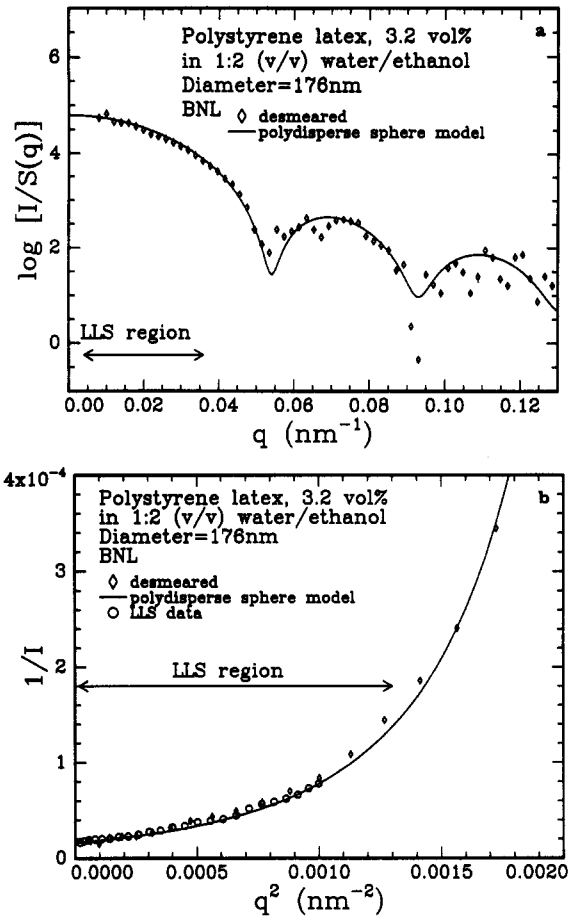

Figure 1. (a) USAXS profile of a Dow Chemical polystyrene latex suspension. (b) Zimm plot of the USAXS profile and the static light scattering results. The desmeared USAXS profile has been corrected for the structure factor ($S(q)$). The concentration used for light scattering measurements is 4×10^{-7} g/mL, and the structure factor correction is negligible. The polydisperse sphere model was computed based on the particle size distribution obtained from dynamic light scattering and CONTIN analysis. We measured the autocorrelation function $G^{(2)}(\tau,q)$, which is related to the first-order scattered electric field time correlation function $g^{(1)}(\tau,q)$ by the relation $G^{(2)}(\tau,q)=A+B|g^{(1)}(\tau,q)|^2$ where τ is the delay time, A is the background, and B is a fitting constant. The normalized distribution of line width Γ at q, $G(\Gamma,q)$, could be obtained by using CONTIN analysis based on the relation $|g^{(1)}(\tau,q)| = \int G(\Gamma,q) \exp(-\Gamma(q)\tau)\, d\Gamma$. The distribution as a function of Γ can be transferred into a size distribution with R being the apparent radius of the latex sphere by using the relations $\Gamma(q) \approx \lim_{q\to 0} Dq^2$ and $D = k_B T/(6\pi\eta R)$ at infinite dilution, where D, k_B, T, and η are respectively the translational diffusion coefficient at infinite dilution and $q \to 0$, the Boltzmann constant, the absolute temperature, and the solvent viscosity. The form factor is then calculated based on the size distribution. More details can be found in ref 62.

The performance of the Bonse–Hart camera at high q values was tested by using an ionomer sample and a conventional Kratky SAXS camera.

The USAXS experiments on the ionomers were performed at our SAXS facility at Stony Brook, using an Enraf-Nonius rotating-anode X-ray generator.

High-Temperature Bonse–Hart USAXS Camera. The details of our high-temperature Bonse–Hart camera have been described in ref 22. The camera used the same set of germanium channel-cut crystals as in the room-temperature Bonse–Hart camera. The mechanical elements were made of super Invar in order to minimize the thermal expansion effects. The instrument permitted us to perform the measurements at temperatures as high as 400 °C and to interchange with temperature jump setups that were developed for our Kratky SAXS instruments. The camera was tested by using the same procedure as described for the room-temperature Bonse–Hart camera. The USAXS experiments on ionomers were performed at NSLS.

The desmearing of Bonse–Hart USAXS data was performed by using a program from Professor Paul Schmidt, University of Missouri—Columbia.

Kratky SAXS Camera. SAXS experiments were performed by using our SAXS facility at Stony Brook. The X-ray beam from an Enraf-Nonius rotating-anode X-ray generator was monochromatized at 0.154 nm by using a Ni filter along with a proportional counter and pulse-height discriminator. Desmearing was performed by using a program which was based on the algorithm developed by Lake.[26]

Procedures for Data Treatment. The procedure for data treatment of the USAXS results needs further justification.

The second crystal in the Bonse–Hart camera had a finite width, and the X-ray was collimated only in one direction. The best way to simplify the desmearing problem was to let the instrument simulate a beam geometry close to that of an infinite-slit length. Unfortunately the synchrotron beam was focused. Thus, the infinte-slit-length (horizontal direction) approximation could induce uncertainties at large q values.

The USAXS curves of the ionomers show a very strong upturn which creates an experimental difficulty in data smoothing before the desmearing procedure. The data shown in this work are all experimental data without any smoothing treatment. Consequently, all small fluctuations in the experimental data were magnified. Furthermore, for such USAXS profiles, the termination error due to desmearing could not be neglected. Some end points had to be truncated.

The absorption correction was another general problem which had not been resolved properly. The normal USAXS absorption correction procedure could be summarized as follows. The intensities at zero scattering angle, i.e., $I(q=0)$, for the sample and the reference (e.g., air, or H-SPS in this work) were matched at $q = 0$, and then the reference curve was subtracted from the sample curve. However, such a procedure implies that the *scattered* intensity of the sample is zero at $q = 0$, which was obviously incorrect in the present study, because the scattered intensity could be a significant portion of the measured total intensity at $q \approx 0$ with the aperture being finite. As an approximation, such a procedure is acceptable in the q region where the excess scattered intensity is much greater than the reference intensity. Then, background subtraction is no longer a critical issue. Thus, we truncated the data points in or close to the q region of the rocking curve ($q < 0.004$ nm^{-1}), and intentionally adjusted the absorption coefficient (by a factor of about 10%) to make sure that the excess scattered intensity did not show detectable changes due to such an adjustment. More details are described in ref 21.

For this work, the scattered intensity of pure polystyrene and that of H-SPS were very close to the air background and were much lower than that of the ionomer samples. Therefore, we used H-SPS-4.5 as a reference. The net USAXS curves remained essentially the same whether we used polystyrene or H-SPS-4.5.

On the basis of the above consideration, we emphasize that the data points presented in this paper could have a relative uncertainty as high as ~10%, particularly at the two ends of the USAXS and SAXS curves.

Results and Discussion

Figure 2 shows the raw USAXS profiles from air, polystyrene, H-SPS-4.5, and Zn-SPS-7.4. Both polystyrene and H-SPS-4.5 show weaker upturns. We can hardly observe any difference between them and the air background. However, we did find a net excess scattered intensity from the samples (PS and H-SPS-4.5) if a synchrotron source was used, as had been reported in ref 22. Similar upturns from other polymers have been reported by several research groups.[27-29]

The scattered intensity of Zn-SPS-7.4 is very strong when compared with that of the pure polystyrene or H-SPS-4.5. This means that the upturn is due mainly to the metal cations. On the basis of the anomalous SAXS results, the contributions due to voids and/or parasitic scattering could be excluded.

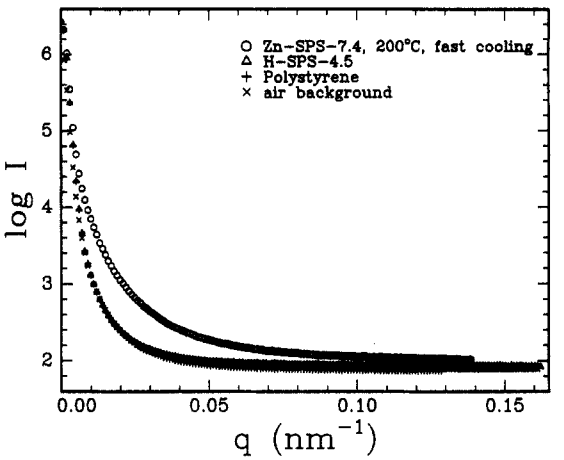

Figure 2. Raw USAXS profiles measured at room temperature. The Zn-SPS-7.4 sample was compression-molded at 200 °C and fast cooled to room temperature (~3 min).

In the previous Communication,[23] we indicated that the Bonse–Hart camera employing a synchrotron X-ray beam did not follow a perfect infinite-slit-length geometry. Although the deviation from the infinite-slit-length approximation was small, certain plots, like the Debye–Bueche plot ($I^{-n} \sim q^2$), could show some deviation at high q values in the desmearing procedure by means of an infinite-slit-length approximation.

The Debye–Bueche model is expressed by[30]

$$I(q) = I(0)/(1 + q^2\xi^2)^2 \quad (1)$$

with $I(0)$ being the I value at $q = 0$ and ξ the inhomogeneity length. The observed deviation reported in the previous Communication[23] could possibly be due to the focusing characteristics of the synchrotron beam. Consequently, we expect the Bonse–Hart camera employing a conventional unfocused X-ray source should give us a geometry which is closer to that of the infinite-slit length as has been discussed by Gravatt and Brady.[31] Figure 3 shows the desmeared and background-corrected USAXS results of the same ionomer sample used in ref 23. The results from the experiment using a conventional X-ray source which could be approximated more closely to an infinite-slit-length geometry indeed showed less deviation when compared with the Kratky SAXS results. Nevertheless, the Debye–Bueche model showed a consistent gentle curvature down to $q = 0.004$ nm^{-1}. On the basis of the Debye–Bueche model, it was difficult to estimate the inhomogeneity length in view of the downward curvature. An estimation of the inhomogeneity length from Figure 3 yielded a value of 130 nm by using a q range from 0.004 to 0.045 nm^{-1} and a value of 40 nm by using a q range from 0.045 to 0.12 nm^{-1}. The values clearly suggest the problem of determining an intercept from a curve with a downward curvature. Previous experiments over higher q ranges would clearly underestimate the magnitude of the inhomogeneity length ξ.

The Debye–Bueche plots for other ionomers show similar shape, although different samples had different scattered intensity.

For a particulate system with negligible particle–particle interaction, the Guinier law[32] can be used to obtain the radius of gyration (R_g) of the particles with

$$I(q) = I(q=0) \exp(-R_g^2 q^2/3) \quad (2)$$

Figure 4 shows a typical Guinier plot for the ionomer Zn-SPS-7.4. Guinier plots of other ionomer samples are similar to Figure 4. The strong curvature clearly suggested

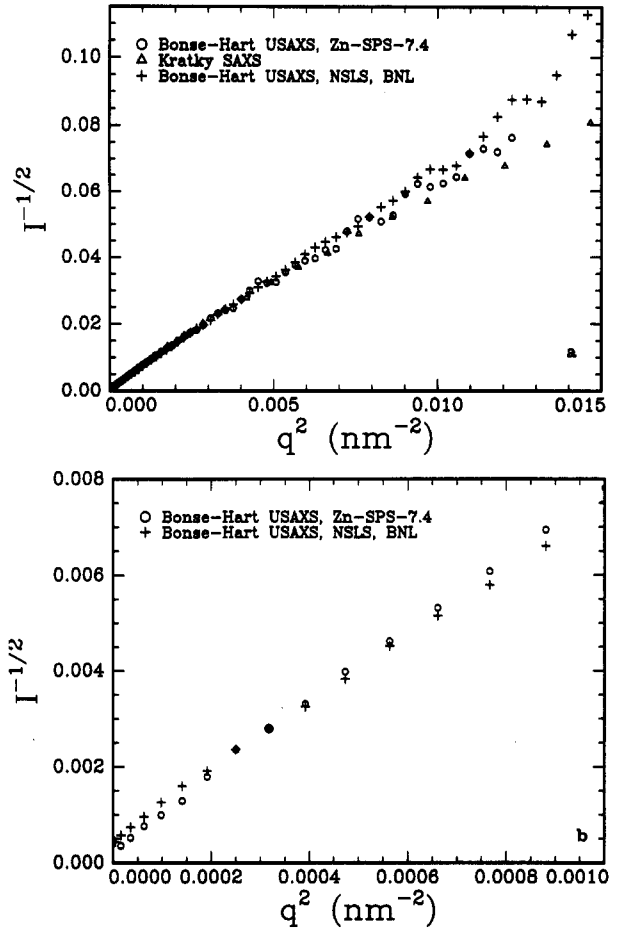

Figure 3. (a and b) Debye–Bueche plot of the desmeared USAXS profile and the Kratky SAXS profile of the ionomer sample used in the previous Communication.[23]

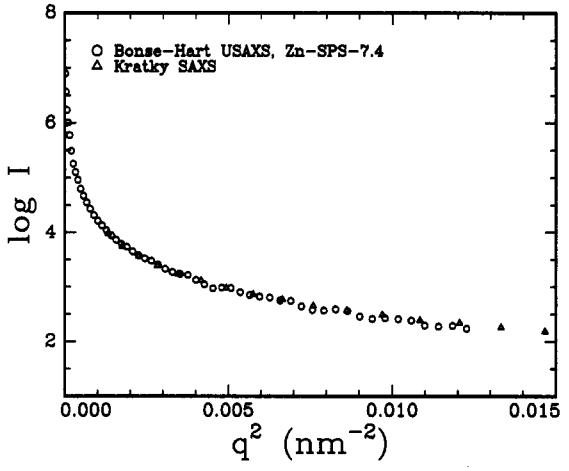

Figure 4. Guinier plot of the USAXS profile and the Kratky SAXS profile of the ionomer sample used in the previous Communication.[23]

that we could not deduce a simple characteristic length from the data. From the initial slope, R_g could be estimated to be about 120–160 nm by fitting the q range from 0.004 to 0.026 nm^{-1} and about 25–28 nm by fitting the q range from 0.055 to 0.12 nm^{-1} for all the ionomers.

Parts a–e of Figure 5 show composite plots of USAXS and SAXS of the ionomer samples. The USAXS curves were shifted to match the SAXS curves. However, only one single shift constant (21 in this case) was used for all the curves. The slight mismatch between the high q tail of the USAXS curves and low q end of the SAXS curves was due to the termination error in the desmearing procedure.

Table I. Power-Law Exponent α ($I \sim q^{-\alpha}$) of the Ionomers (Fitting Region 0.004–0.5 nm^{-1})

sample	α
Na-SPS-10.9	2.9
Rb-SPS-11.4	2.4
Rb-SPS-13.0	2.6
Zn-SPS-2.9, 200 °C, fast cooling	3.0
Zn-SPS-2.9, 200 °C, slow cooling	3.0
Zn-SPS-7.4, 200 °C, fast cooling	3.6
Zn-SPS-7.4, 200 °C, slow cooling	3.5
Zn-SPS-7.4, 230 °C, slow cooling	3.6
Zn-SPS-13.7, 200 °C, fast cooling	3.5
Zn-SPS-13.7, 200 °C, slow cooling	3.4

It is interesting to note that the shape of the upturn was insensitive to the nature of the cations and the ionic content. Their intensity deserved some discussion. The intensity of the upturn for Rb-SPS-11.4 was higher than that for Na-SPS-10.4 (Figure 5a) as expected because of the higher scattering power of Rb. However, although the intensity of the upturn for Rb-SPS-13.0 was higher than that for Rb-SPS-11.4 (Figure 5a), the intensity of the upturn for Zn-SPS-13.7 was *lower* than that for Zn-SPS-7.4, and the intensity of the upturn for Zn-SPS-2.9 was *higher* than that for Zn-SPS-7.4 at higher q values and *lower* at smaller q values (Figure 5b). On the other hand, the ionic peak was consistently higher for the ionomer samples with higher ionic content, irrespective of the cations. This difference in the dependence of the upturn on the ionic content of Zn and Rb could be due to the fact that Zn formed divalent cations Zn(II) while Rb formed monovalent cations Rb(I). Weiss[33,34] and co-workers also found different dependence on Na- and Zn-SPS samples and suggested[35] that the difference might be explained on the basis of crystal packing. They proposed that the sulfonate anion packing was independent of the cation and that the cluster density for a divalent cation was greater than that for a monovalent cation. The tendency for interaction with the sulfonate anions was more favorable for the monovalent cations. The same argument could apply although no conclusive evidence could be provided.

USAXS and SAXS experiments were also performed on samples which were compression-molded under different conditions. The molding temperature changed from 200 to 230 °C, and the cooling time changed from ~3 min (fast cooling) to ~200 min (slow cooling). We could not see obvious trends with different compression-molding conditions, as shown in parts a–e of Figures 5.

A surprising feature of the composite curves in parts a–e of Figure 5 is that the scattering behavior of the upturn could be described approximately by a power law, $I \sim q^{-\alpha}$, where α is a constant. In most cases, such a power-law scattering behavior could cover as large as 7 orders of magnitude in I space and 2 orders of magnitude in q space.

The fractal structures could give rise to power-law scattering[36–38] which gives us information as to whether the structure is a mass fractal or a surface fractal, as well as the roughness of the fractal. Table I shows the α values for the ionomer samples in this study. As the α values change from 2.4 to 3.6, it is questionable whether the fractal principle should be applied to the data. For the samples with $\alpha > 3.0$, a surface fractal is implied. If it were true, the "pore size" in the samples would be on the order of microns. However, the fractal structure is not the only source which could give a power-law scattering behavior. For example, Schmidt[39] has shown that a power-law distribution of spheres, platelets, or rods could also yield power-law scattering behaviors. At any rate, the power-law scattering behavior suggests at least the following features: the systems are inhomogeneous from the na-

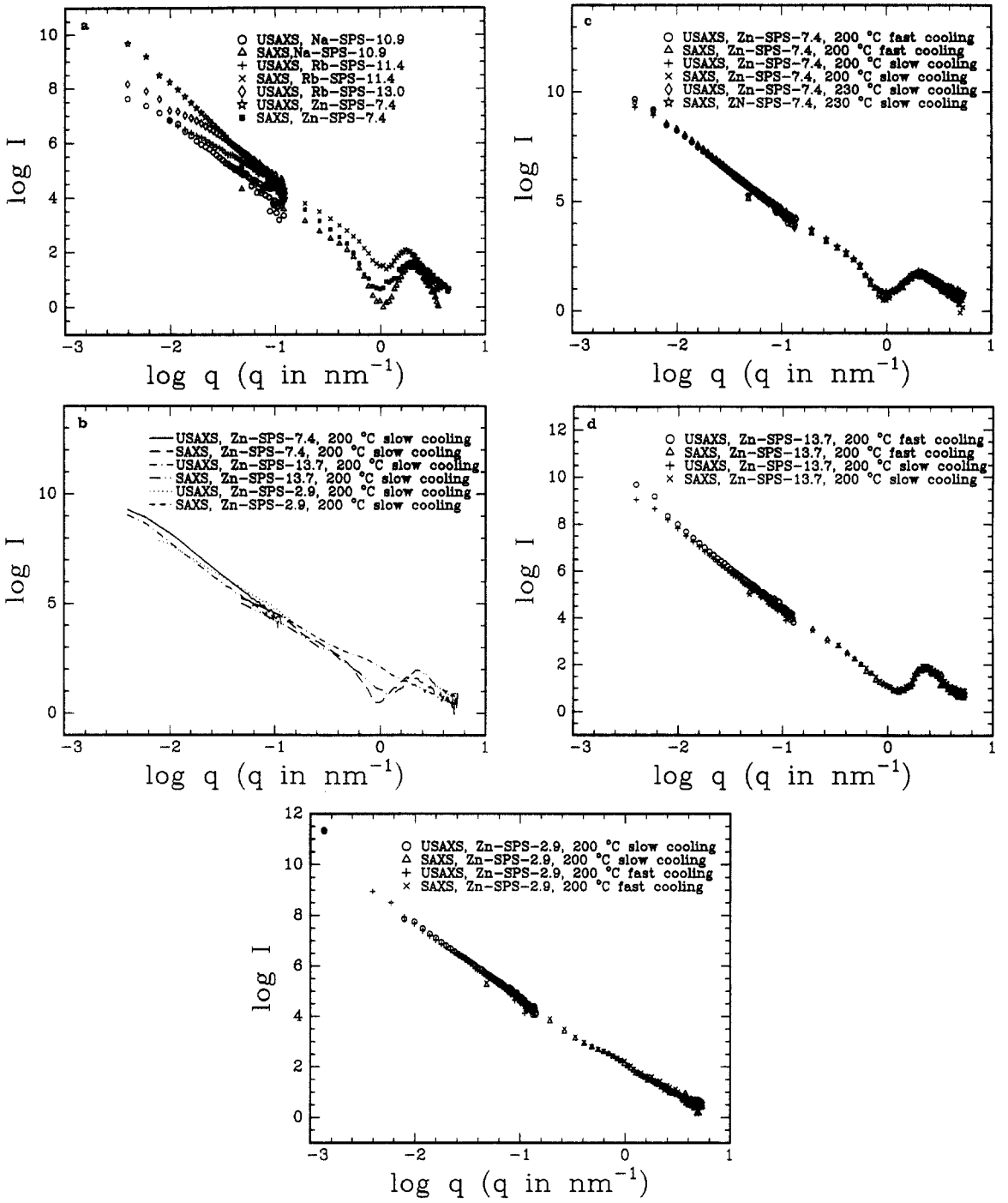

Figure 5. (a–e) Composite plots of USAXS profiles and Kratky SAXS profiles of the ionomer samples. The temperature following the sample names in each part is the molding temperature. The time for fast cooling is ~3 min; the time for slow cooling is ~200 min.

nometer to micron scale; the structure is very polydisperse or very irregular; and the systems do not have a characteristic long-range order.

The effects of annealing and temperature on the structure (SAXS q region) of sulfonated polystyrene ionomers have been studied by several groups.[12,13,33,34,40-48] Weiss and co-workers[34] found annealing at high temperatures of Zn-SPS decreased the integrated scattered intensity, while Yarusso and Copper[40] reported that they observed a change neither in aggregate size nor in concentration of the aggregates from room temperature to 290 °C. Both groups observed that the ionic peak was retained at very high temperatures (above 266 °C). The results from dynamic mechanical analysis of Zn-SPS-5.81 showed two relaxations,[46] one at ~120 °C representing the glass transition of the polymer matrix and the other one at ~200 °C representing the glass transition of the ion-rich domains, the so-called clusters by using the terminology of Eisenberg et al.[20] As the transition at higher temperatures was mainly due to the clusters and the clusters could be related to the USAXS upturn, it should be interesting to investigate the effects of temperature and annealing on the upturn. We used our high-temperature Bonse–Hart USAXS camera[22] employing a synchrotron X-ray source to study the temperature and annealing dependence of the upturn. The synchrotron source was used in order to reduce the measurement time and to minimize any degradation of the ionomer samples at high temperatures. Figure 6 shows the temperature dependence of the USAXS profiles of the ionomer Zn-SPS-7.4 with increasing temperature. At each temperature, we waited for about 20 min before data collection

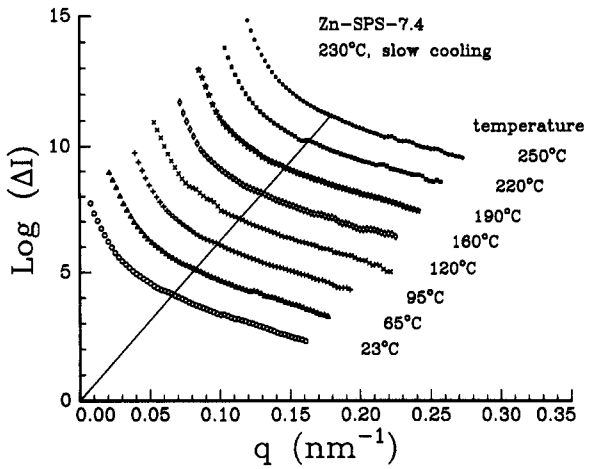

Figure 6. USAXS profiles of a Zn-SPS-7.4 sample measured at different temperatures.

which took another ~30 min to accomplish. A longer time could be needed for the system to reach equilibrium. However, consideration of possible thermal degradation prevented us from annealing the sample over longer time periods. The highest temperature we reached was 250 °C because once again we worried that, at temperatures higher than 250 °C, thermal degradation could become appreciable. Nonetheless, 250 °C was appreciably higher than the reported 200 °C as the glass transition of the ionic domains.

The overall tendency on the temperature dependence of the USAXS profiles was a very slight increase in the scattered intensity with increasing temperature. This slight increase could be due to the difference in the thermal expansion coefficient of the ion-poor phase and the ion-rich phase.[49,50] We did not observe any significant changes in either the angular dependence or the magnitude of the USAXS profiles from 25 to 250 °C. The insensitivity of the upturn to temperature and annealing could be due to the strong cross-linking effects of the ion multiplets, which were stable up to 250 °C. Even above the glass transition of the ion-rich phase, the multiplets could remain intact, and the cluster structure was still locked in due to the high melt viscosity. The whole system remained inhomogeneous. The high-temperature resistent cluster structure could be responsible for the high-temperature properties of the ionomers.

In summary, the key point from our USAXS and SAXS results is that the upturn of the ionomers did not show a strong dependence upon the nature of the cations, the ionic content, the compression-molding conditions, the annealing procedures, and the temperature variations from 25 to 250 °C. On the basis of these results, we believe that the upturn is due to the intrinsic chemical compositional inhomogeneities. The chemical compositional inhomogeneities result from the nonrandom sulfonation reaction as well as neutralization of the acid form; i.e., the polymers were not formed in a homogeneous reaction medium. This suggestion has been supported by our recent experiment on Zn-SPS. When we dissolved some ionomer samples, very often we could observe a nonnegligible insoluble portion, especially at high ionic content. The insoluble portion was separated for further chemical compositional analysis which indicated the insoluble portion to contain a substantially higher amount of Zn. This definitive though crude experiment confirmed that the ionomer samples have severe chemical compositional inhomogeneities. Consequently, polymer chains with different degrees of sulfonation and/or neutralization could have different solubilities in most solvents and the long-range inhomogeneities could start to form when the ionomers were formed in their "solution" state. With increased concentration of the ionomers, the systems could become nonuniform. Concentration fluctuations due to ion-rich and ion-poor, or sulfonation-rich or sulfonation-poor, regions could take place at this stage. Once again, we want to emphasize that the concentration fluctuations are due to the nonuniform compositional distribution of the polymer chains, which has little relation with the well-accepted concepts of ionic multiplets of ionic domains responsible for the ionic peak in SAXS. Yet, the system could become cross-linked due to the formation of multiplets. Then, the nonuniform structure would be locked in by the "ionic cross-links". The topological constraints created by the multiplets could prevent the system from reaching a more uniform state. Conventional processes, such as annealing and compression-molding, could not change the structure appreciably. Therefore, we could not observe any dependence on the upturn by annealing, by changing the compression-molding condition, or by heating to temperatures higher than the glass transition temperature of the ionomers. It might not be difficult to understand the power-law scattering behavior in the ionomers because microphase separation could very likely generate a long-range inhomogeneous structure. The high-temperature resistance to the ionic peak and to the upturn also implied that the sample preparation history before compression-molding would determine the structure after compression molding. From electron spin resonance (ESR) measurements, Galambos et al.[13] showed that the Mn ions in their Mn-SPS-7.6 sample were associated at both 25 and 150 °C, implying that the cross-linked structure could be formed even before compression molding. Once formed, the cross-links would sustain all the remaining processes. In this way, the compression-molding condition would have little effect on the final structure of the ionomers. The structure could be predetermined by the polarity of the solvent used before compression molding,[13,43-45] as the polarity of the solvent had controlling effects on the structure of ionomers from solution-casting or even in dilute solution.[24,43,45,51-61]

The upturn in the small q region is not a new topic and has been observed in almost all kinds of polymers.[27-29,63-65] Generally, "pure" organic homopolymers showed an upturn, even in the melt state.[63] The small-angle upturn was found to be due mainly to foreign particles and could not be attributed to the inherent structure in the pure polymer amorphous phase.[27] Although the amount of such foreign particles could be small, in many cases the electron density contrast between the foreign particles and the polymers was large. Consequently, the small-angle upturn was high. Purification of the homopolymers could drastically reduce the small-angle upturn, especially if one were to follow the clarification procedures used in light scattering techniques and annealed the melt very slowly so as to produce a strain-free sample. For ionomers, the neutralization process involved the use of metallic compounds. Therefore, even if there were no chemical compositional inhomogeneities, the contribution of foreign particles to the upturn should be difficult to avoid.

Conclusion

Two newly constructed and tested Bonse–Hart cameras were used to study the USAXS upturn of ionomers. The Debye–Bueche model showed a marginal fitting of the USAXS curves. A consistent curvature was observed down to the q range previously accessible only by means of light

scattering. Based on the Debye–Bueche model, the inhomogeneity length was on the order of a tenth of a micron, depending upon the q region used. The Guinier plot also failed to yield a single characteristic length. The shape of the upturn did not show a strong dependence upon the nature of the cations, the ionic content, the compression-molding condition, the annealing procedure, and temperature variations from 25 to 250 °C. The upturn could be described approximately by a power-law scattering behavior, suggesting an inhomogeneous structure varying in length scales from nanometers to about a micron. The intrinsic chemical compositional inhomogeneities and the processing procedure could be the reasons for the nonuniformity in structure as revealed by the SAXS small-angle upturn.

Acknowledgment. B.C. acknowledges the financial support of this project by the U.S. Department of Energy (Grants DEFG0286ER45237.A008 and DEFG0589-ER75515). Y.L. thanks Eugene Sokolov for the desmearing program and Professor Zukang Zhou for the light scattering measurement.

References and Notes

(1) Eisenberg, A., Ed. *Ions in Polymers*; Advances in Chemistry Series 187; American Chemical Society: Washington, DC, 1980.
(2) MacKnight, W. J.; Earnest, T. R., Jr. *J. Polym. Sci., Macromol. Rev.* **1981**, *16*, 41.
(3) Pineri, M., Eisenberg, A., Eds. *Structure and Properties of Ionomers*; NATO Advanced Study Institute Series 198; Reidel: Dordrecht, Holland, 1987.
(4) Fitzgerald, J. J.; Weiss, R. A. *J. Macromol. Sci., Rev. Macromol. Chem. Phys.* **1988**, *C28*, 99.
(5) Tant, M.; Wilkes, G. L. *J. Macromol. Sci., Rev.* **1988**, *C28*, 1.
(6) Mauritz, K. A. *J. Macromol. Sci., Rev.* **1988**, *C28*, 65.
(7) MacKnight, W. J.; Taggart, W.; Stein, R. S. *J. Polym. Sci., Polym. Symp. Ed.* **1973**, *45*, 113.
(8) Yarusso, D. J.; Cooper, S. L. *Macromolecules* **1983**, *16*, 1871.
(9) Visser, S. A.; Cooper, S. L. *Macromolecules* **1991**, *24*, 2584.
(10) Dreyfus, B.; Gebel, G.; Aldebert, P.; Pineri, M.; Excoubes, M.; Thomas, M. *J. Phys. Fr.* **1990**, *51*, 1341.
(11) Register, R. A. Ph.D. Thesis, University of Wisconsin—Madison, Madison, WI, 1989.
(12) Williams, C. E.; Russell, T. P.; Jerome, R.; Horrion, J. *Macromolecules* **1986**, *19*, 2887.
(13) Galambos, A. F.; Stockton, W. B.; Koberstein, J. T.; Sen, A.; Weiss, R. A.; Russell, T. P. *Macromolecules* **1987**, *20*, 3094.
(14) Ding, Y. S.; Hubard, S. R.; Hodgson, K. O.; Register, R. A.; Cooper, S. L. *Macromolecules* **1988**, *21*, 1698.
(15) Wu, D. Q.; Phillips, J. C.; Lundberg, R. D.; MacKnight, W. J.; Chu, B.; *Macromolecules* **1989**, *22*, 992. Wu, D. Q. Ph.D. Thesis, SUNY at Stony Brook, 1989.
(16) Register, R. A.; Cooper, S. L. *Macromolecules* **1990**, *23*, 310.
(17) Moore, R. B.; Gauthier, M.; Williams, C. E.; Eisenberg, A. *Macromolecules* **1992**, *25*, 5769.
(18) Chu, B.; Wu, D. Q.; Lungberg, R. D.; MacKnight, W. J. *Macromolecules* **1993**, *26*, 994. Wu, D. Q.; Chu, B.; Lundberg, R. D.; MacKnight, W. J. *Macromolecules* **1993**, *26*, 1000.
(19) Kumar, S.; Pineri, M. *J. Polym. Sci., Polym. Phys. Ed.* **1986**, *24*, 1767.
(20) Eisenberg, A.; Hird, B.; Moore, R. B. *Macromolecules* **1990**, *23*, 4098.
(21) Chu, B.; Li, Y.; Gao, T. *Rev. Sci. Instrum.* **1992**, *63*, 4128.
(22) Chu, B.; Li, Y.; Harney, P. J.; Yeh, F. *Rev. Sci. Instrum.*, in press.
(23) Chu, B.; Wang, J.; Li, Y.; Peiffer, D. G. *Macromolecules* **1992**, *25*, 4229.
(24) Lungberg, R. D.; Makowski, H. S. *J. Polym. Sci., Polym. Phys. Ed.* **1980**, *18*, 1821.
(25) Vrij, A.; Jansen, J. W.; Dhont, J. K. G.; Pathmamanoharan, C.; Kops-Werkhoven, M. M.; Funat, H. M. *Faraday Discuss. Chem. Soc.* **1983**, *76*, 19.
(26) Lake, J. A. *Acta Crystallogr.* **1967**, *23*, 191.
(27) Wendorff, J. H.; Fischer, E. W. *Kolloid Z. Z. Polym.* **1973**, *251*, 884.
(28) Lin, W.; Kramer, E. J. *J. Appl. Phys.* **1973**, *44*, 4288.
(29) Renninger, A. L.; Wicks, G. G.; Uhlmann, D. R. *J. Polym. Sci., Polym. Phys. Ed.* **1975**, *13*, 1247. Renninger, A. L.; Uhlmann, D. R. *J. Polym. Sci., Polym. Phys. Ed.* **1975**, *13*, 1481; **1976**, *14*, 415. Straff, R. S.; Uhlmann, D. R. *J. Polym. Sci., Polym. Phys. Ed.* **1976**, *14*, 353. Renninger, A. L.; Uhlmann, D. R. *J. Polym. Sci., Polym. Phys. Ed.* **1978**, *16*, 2237. Matyi, R. J.; Uhlmann, D. R. *J. Polym. Sci., Polym. Phys. Ed.* **1980**, *18*, 1053.
(30) Debye, P.; Bueche, A. M. *J. Appl. Phys.* **1949**, *20*, 518. Debye, P.; Anderson, H. R.; Brumberger, H. *J. Appl. Phys.* **1957**, *28*, 679.
(31) Gravatt, C. C.; Brady, G. W. *J. Appl. Crystallogr.* **1969**, *2*, 289.
(32) Guinier, A.; Fournet, G. *Small-Angle Scattering of X-rays*; Wiley: New York, 1955.
(33) Weiss, R. A.; Lefelar, J. A.; Toriumi, H. *J. Polym. Sci., Polym. Lett. Ed.* **1983**, *21*, 661.
(34) Weiss, R. A.; Lefelar, J. A. *Polymer* **1986**, *27*, 3.
(35) Lefelar, J. A.; Weiss, R. A. *Macromolecules* **1984**, *17*, 1145.
(36) Martin, J. E.; Hird, A. J. *J. Appl. Crystallogr.* **1987**, *20*, 61.
(37) Avnir, D., Ed. *The Fractal Approach to Heterogeneous Chemistry*; Wiley: Chichester, England, 1989.
(38) Schmidt, P. W. *J. Appl. Crystallogr.* **1991**, *24*, 414.
(39) Schmidt, P. W. *J. Appl. Crystallogr.* **1982**, *15*, 567.
(40) Yarusso, D. J.; Cooper, S. L. *Polymer* **1985**, *26*, 371.
(41) Weiss, R. A. *J. Polym. Sci., Polym. Phys. Ed.* **1982**, *20*, 65.
(42) Toriumi, H.; Weiss, R. A.; Frank, H. A. *Macromolecules* **1984**, *17*, 2104.
(43) Fitzgerald, J. J.; Kim, D.; Weiss, R. A. *J. Polym. Sci., Polym. Lett. Ed.* **1986**, *24*, 263.
(44) Register, R. A.; Sen, A.; Weiss, R. A.; Cooper, S. L. *Macromolecules* **1989**, *22*, 2224.
(45) Fitzgerald, J. J.; Weiss, R. A. *J. Polym. Sci., Polym. Phys. Ed.* **1990**, *28*, 1719.
(46) Rigdahl, M.; Eisenberg, A. *J. Polym. Sci., Polym. Phys. Ed.* **1981**, *19*, 1641.
(47) Weiss, R. A.; Fitzgerald, J.; Kim, D. *Macromolecules* **1991**, *24*, 1071.
(48) Wang, J.; Li, Y.; Peiffer, D. G.; Chu, B. *Macromolecules* **1993**, *26*, 2633.
(49) Fischer, E. W.; Kloos, F.; Lieser, G. *J. Polym. Sci., Polym. Lett. Ed.* **1969**, *7*, 845.
(50) Fischer, E. W. *Pure Appl. Chem.* **1971**, *26*, 385.
(51) Lungberg, R. D.; Phillips, R. R. *J. Polym. Sci., Polym. Phys. Ed.* **1982**, *20*, 1143.
(52) Hara, M.; Wu, J. L. *Macromolecules* **1986**, *19*, 2887.
(53) Hara, M.; Lee, A. H.; Wu, J. *J. Polym. Sci., Polym. Phys. Ed.* **1987**, *25*, 1407.
(54) Weiss, R. A.; Fitzgerald, J. J.; Frank, H. A.; Chadwick, B. W. *Macromolecules* **1986**, *19*, 2085.
(55) Lantman, C. W.; MacKnight, W. J.; Peiffer, D. G.; Sinha, S. K.; Lundberg, R. D. *Macromolecules* **1987**, *20*, 1096.
(56) Hara, M.; Wu, J. L. *Macromolecules* **1988**, *21*, 402.
(57) Lantman, C. W.; MacKnight, W. J.; Peiffer, D. G.; Sinha, S. K.; Lundberg, R. D. *Macromolecules* **1988**, *21*, 1339.
(58) Lantman, C. W.; MacKnight, W. J.; Peiffer, D. G.; Sinha, S. K.; Lundberg, R. D. *Macromolecules* **1988**, *21*, 1344.
(59) Gabrys, B.; Higgins, J. S.; Lantman, C. W.; MacKnight, W. J.; Pedley, A. M.; Peiffer, D. G.; Rennie, A. R. *Macromolecules* **1989**, *22*, 3746.
(60) Pedley, A. M.; Higgins, J. S.; Peiffer, D. G.; Burchard, W. *Macromolecules* **1990**, *23*, 1434.
(61) Pedley, A. M.; Higgins, J. S.; Peiffer, D. G.; Rennie, A. R. *Macromolecules* **1990**, *23*, 2494.
(62) Chu, B. *Laser Light Scattering: basic principles and practice*; Academic Press: Boston, 1991.
(63) Kortleve, G.; Tuijnman, C. A. F.; Vonk, C. G. *J. Polym. Sci., Polym. Phys. Ed.* **1972**, *10*, 123.
(64) Fischer, E. W.; Dettenmaier, M. *J. Non-Cryst. Solids* **1978**, *31*, 181.
(65) Koike, Y.; Tanio, N.; Ohtsuka, Y. *Macromolecules* **1989**, *22*, 1367.